



HAL
open science

Ultrafast Spin Crossover Photochemical Mechanism in [Fe II (2,2'-bipyridine) 3] 2+] Revealed by Quantum Dynamics

Marc Alías-Rodríguez, Swarnendu Bhattacharyya, Miquel Huix-Rotllant

► **To cite this version:**

Marc Alías-Rodríguez, Swarnendu Bhattacharyya, Miquel Huix-Rotllant. Ultrafast Spin Crossover Photochemical Mechanism in [Fe II (2,2'-bipyridine) 3] 2+] Revealed by Quantum Dynamics. Journal of Physical Chemistry Letters, 2023, 14 (38), pp.8571-8576. 10.1021/acs.jpcllett.3c02201 . hal-04291627

HAL Id: hal-04291627

<https://hal.science/hal-04291627>

Submitted on 17 Nov 2023

HAL is a multi-disciplinary open access archive for the deposit and dissemination of scientific research documents, whether they are published or not. The documents may come from teaching and research institutions in France or abroad, or from public or private research centers.

L'archive ouverte pluridisciplinaire **HAL**, est destinée au dépôt et à la diffusion de documents scientifiques de niveau recherche, publiés ou non, émanant des établissements d'enseignement et de recherche français ou étrangers, des laboratoires publics ou privés.

Ultrafast Spin Crossover Photochemical Mechanism in $[\text{Fe}^{\text{II}}(2,2'\text{-bipyridine})_3]^{2+}$ Revealed by Quantum Dynamics

Marc Alías-Rodríguez,^{†,‡} Swarnendu Bhattacharyya,^{†,‡} and Miquel Huix-Rotllant^{*,†}

[†]*Aix-Marseille Univ, CNRS, ICR, Marseille, 13013, France.*

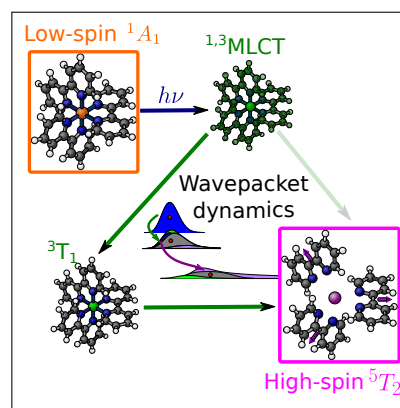
[‡]*Contributed equally to this work*

E-mail: miquel.huix-rotllant@cnr.fr

Abstract

Photoexcitation of $[\text{Fe}^{\text{II}}(2,2'\text{-bipyridine})_3]^{2+}$ induces a sub-picosecond spin crossover transformation from a low-spin singlet to a high-spin quintet state. The mechanism involves metal-centered (MC) and metal-ligand charge transfer (MLCT) triplet intermediates, but their individual contributions to this efficient intersystem crossing ~~are still unclear~~ have been object of debate. Employing quantum wavepacket dynamics, we show that MC triplets are catalyzing the transfer to the high-spin state. This photochemical pathway is made possible thanks to bipyridine stretching vibrations, facilitating the conversion between the MLCT bands to such MC triplets. We show that the lifetime of the MLCT states can be increased to tens of picoseconds by breaking the conjugation between pyridine units, which increases the energetic gap between MLCT and MC states. This opens the route for the design of new chelating ligands inducing long-lived MLCT states in iron complexes.

TOC Graphic



Molecules containing d^4 to d^7 octahedral metal complexes exhibit magnetic bistability known as spin crossover (SCO), in which the metal center undergoes a transition from a low-spin (LS) to a high-spin (HS) electronic configuration, induced by several kinds of external stimuli such as temperature, pressure, light radiation or the application of a magnetic field.^{1–8} Light-induced SCO reactions (commonly known as light-induced excited spin-state trapping, LIESST) have attracted particular interest. Such photoactive complexes can act as molecular switches due to the ultrafast conversion between two magnetic states.⁹ Conversely, efficient light-harvesting and photocatalyst complexes can be produced by delaying the SCO reaction which stabilizes charge-transfer states.¹⁰ The photochemical pathways are highly dependent on the type of metal, the ligands, the electronic band structure, and the initial absorbing state.⁹ Elucidating the LIESST mechanisms is fundamental for designing complexes with controlled photoreactivity.

The current understanding of LIESST mechanisms is in most cases incomplete, especially due to the complex interplay between electronic and vibrational degrees of freedom and the ultrafast nature of the photoreaction, which challenges the interpretation of time-resolved spectra.^{3–8,11–18} Theoretical models, on the other hand, can only provide a complete model for the photoreaction when a balanced treatment of non-adiabatic and spin-orbit couplings of electronic excited states with different spin multiplicities is used, requiring state-of-the-art methodologies for electronic structure and quantum dynamics.¹⁹ Multi-configuration time-dependent Hartree (MCTDH) wavepacket dynamics, pioneered by Pápai and Penfold, have been shown to successfully describe the photophysics of iron complexes.^{20–23}

The LIESST reactions in organometallic iron compounds have been the focus of much research, due to the cost-effectiveness and scalability of iron complexes.²⁴ In the present study, we focus on the LIESST mechanism of a well-known iron complex, $[\text{Fe}(\text{bpy})_3]^{2+}$ (bpy=2,2'-bipyridine) (see Fig. 1). The low-spin (LS) state of $[\text{Fe}(\text{bpy})_3]^{2+}$ corresponds to a singlet closed-

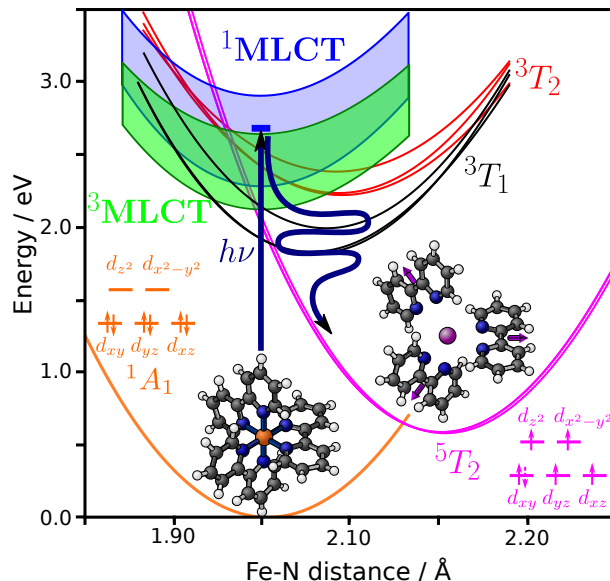


Figure 1: Representation of the potential energy surfaces and geometric changes during LIESST reaction in $[\text{Fe}(\text{bpy})_3]^{2+}$, including the high-spin (5T_2), the metal-centered triplets (3T_1 and 3T_2) and the singlet/triplet metal-ligand charge transfer states ($^1/{}^3MLCT$).

shell configuration (1A_1), in which six nitrogens form a dative covalent bond with the iron center. The high-spin (HS) states are constituted by a quintet triad (5T_2) with a gap of ca. 0.1 eV due to a small Jahn-Teller distortion.²⁵ According to our simulations, the HS is characterized by a symmetric increase of the Fe-N distances (+0.2 Å) and a slight decrease (-5.7°) of the N-Fe-N bite angle with respect to the LS equilibrium geometry. This is a consequence of populating e_g antibonding orbitals. The absorption spectrum exhibits two maximum absorbances at 520 and 350 nm corresponding to metal-to-ligand-charge-transfer (MLCT) states.^{13,14,26,27}

The photochemical LIESST mechanism in $[\text{Fe}(\text{bpy})_3]^{2+}$ has been thoroughly studied both experimentally and theoretically.^{3–8,13–18} The $[\text{Fe}(\text{bpy})_3]^{2+}$ photoreaction model depicted by time-resolved spectroscopy has been refined in parallel to the development of new techniques with improved time resolution.^{11,28} One of the first studies employing UV-visible transient absorption spectroscopy suggested a sub-ps $^1MLCT \rightarrow ^5T_2$.²⁹ Time-resolved fluorescence spectroscopy of Gawelda et al. pointed out the population transfer between MLCT states

($^1\text{MLCT} \rightarrow ^3\text{MLCT}$) in 15 fs,³ and mechanism via the MC triplets ($^3\text{MLCT} \rightarrow ^3\text{MC}$) in 120 fs prior to the HS transfer in 960 fs. This mechanism was confirmed and refined by Gaffney and coworkers using time-resolved X-ray K_β fluorescence spectroscopy, with 150 fs MLCT/MC triplet transfer and a faster transfer to quintets in 70 fs.⁶ Combining time-resolved X-ray emission and scattering, Gaffney et al. later indicated that HS \rightarrow ^3MC back-transfer occurs prior to the final relaxation to the HS.¹¹ Auböck and Chergui, based on high-resolution UV-visible pump-probe spectroscopy determined a build-up of HS population in less than 50 fs, assisted by high-frequency ligand modes.⁷ Lemke et al. confirmed this mechanism using time-resolved X-ray absorption spectroscopy estimating a slower transfer rate of 120 fs to the HS.⁸ Finally, Moguilevski et al. using ultrafast extreme UV photoemission spectroscopy determined that both $^3\text{MC} \rightarrow \text{HS}$ and $^3\text{MLCT} \rightarrow \text{HS}$ were competing mechanisms.³⁰ From a theoretical perspective, there is no unified model of the mechanism of $[\text{Fe}(\text{bpy})_3]^{2+}$ photoreaction. Sousa et al. computed the kinetic rates of intersystem crossing (ISC) using Fermi’s golden rule, determining a dominant $^3\text{MC} \rightarrow \text{HS}$ mechanism due to larger MC/HS spin-orbit coupling,¹⁵ but later considered the direct $^3\text{MLCT} \rightarrow \text{HS}$ mechanism possible from the mixing between MC and MLCT states due to thermal disorder.¹⁶ Iuchi et al. have recently presented a trajectory surface hopping study in $[\text{Fe}(\text{bpy})_3]^{2+}$ in aqueous solution using a constructed model Hamiltonian, proposing a dominant SCO transfer via ^3MC states.³¹

We construct a complete quantum dynamics model for describing the LIESST reaction in $[\text{Fe}(\text{bpy})_3]^{2+}$ describing the SCO photodynamics upon absorption to the bright states within the MLCT band. The details of the construction of the model can be found in the Supporting Information (see further in Sec. S2). The model contains the lowest part of the excited state spectrum, which can be characterized either by d-d type transitions (MC states) or a d- to π_1^* bipyridine orbitals (MLCT states), composed of a $\text{C}_2\text{-C}_{2'}$ bonding π region and a $\text{N-C}_2/\text{N-C}_{2'}$ anti-bonding π^* region common of

diimine bonds (see Fig. S1 and S2). In the D_3 geometry, the π^* orbitals have an $\text{a}_2 \oplus \text{e}$ symmetry delocalized over the three equivalent bipyridine units. The singlet bright states are found in the middle of the MLCT band and have $t_{2g} \rightarrow \pi_1^*$ character, using the O_h notation. The excitation at the $^1\text{A}_1$ minimum geometry is 2.65 eV, with an oscillator strength of $8.5 \cdot 10^{-2}$ a.u. The rest of the singlet MLCT band is dark. The $^1\text{T}_1$ states lie at the upper end of the MLCT band (around 3 eV) and are not accessible from the lower range of the absorption spectrum. The triplet manifold consists of an MLCT band (2.09-2.51 eV) overlapping with the $^1\text{MLCT}$ band, the ^3MC , and the $^5\text{T}_2$ states. The $^3\text{T}_1$ is found in a range of 1.91-2.13 eVs, while the $^3\text{T}_2$ lies between 2.41-2.62 eV. These excited state energies are computed along 9 vibrational modes (see SI): (i) the reaction coordinate (depicted in Fig. 1) consisting mainly of a symmetric stretching of all Fe-N distances, (ii) two Jahn-Teller asymmetric Fe-N stretching modes that distort the complex in axial/equatorial planes, and (iii) six ligand centered modes corresponding to a $\text{C}_2\text{-C}_{2'}$ coupled with C-C and C-N inter-ring stretching modes of the bipyridine units accounting for the relaxation in the MLCT bands.

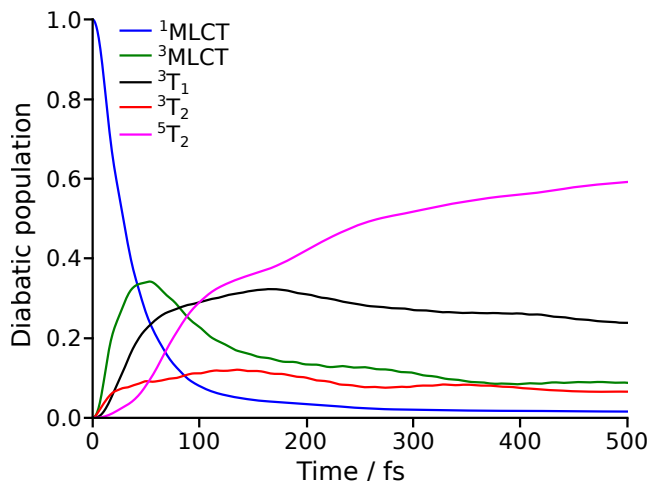


Figure 2: Diabatic population dynamics of $^1,^3\text{MLCT}$, $^1,^3\text{MC}$ ^3MC ($^3\text{T}_1$ and $^3\text{T}_2$) and HS ($^5\text{T}_2$) states during the first 0.5 ps using the full hamiltonian model of $[\text{Fe}(\text{bpy})_3]^{2+}$. The singlet $^1\text{T}_1$ is included in the model, but not depicted in the figure due to negligible population.

The vibronic model has been used in quantum dynamics starting from a wavepacket in the lowest bright $^1\text{MLCT}$ states. The results for the first 0.5 ps are shown in Fig. 2. The population on the $^1\text{MLCT}$ undergoes a rapid decay becoming negligible after 150 fs. The first decay of the $^1\text{MLCT}$ is concomitant to the rapid growth of the $^3\text{MLCT}$ population, which becomes dominant at around 50 fs. The wavepacket is then split into three different populations. The dynamic evolution of populations of the two ^3MC states behaves similarly. On the one hand, the $^3\text{T}_1$, which receives 30% of the population, exhibits a rapid growth from the beginning of the dynamics followed by a slow decay after 150 fs. On the other hand, the $^3\text{T}_2$, which receives 10% of the population has a slow decay after 100 fs. The quintet $^5\text{T}_2$ has a rapid and steady growth starting at around 50 fs until the end of the dynamics, becoming the dominant population after around 120 fs.

The triplet intermediates ($^3\text{MLCT}$, $^3\text{T}_1$ and $^3\text{T}_2$) have been experimentally observed during the SCO photodynamics,^{7,8,10,30} but there is a debate on which triplet catalyzes the intersystem crossing to the HS state. Indeed, two types of intersystem crossing mechanisms can be distinguished, either via a direct intersystem crossing (“direct mechanism”, $^3\text{MLCT} \rightarrow \text{HS}$) or a triplet internal conversion prior to the intersystem crossing (“indirect mechanism”, $^3\text{MLCT} \rightarrow ^3\text{MC} \rightarrow \text{HS}$). In order to unravel the mechanism, we performed wavepacket dynamics on “reduced” model Hamiltonians, in which we deactivate certain interstate couplings or vibrational modes, allowing us to dissect the dominant pathways in the excited state.

The evolutions of diabatic populations from the wavepacket dynamics on reduced models are shown in Fig. 3. At first glance, the dynamics deactivating the $^3\text{MLCT}$ - $^5\text{T}_2$ spin-orbit coupling are equal to the full model. In contrast, the HS state is not populated when deactivating the ^3MC - $^5\text{T}_2$ spin-orbit coupling. This excludes the possibility of a “direct mechanism”, in agreement with the weak spin-orbit coupling between $^3\text{MLCT}$ and $^5\text{T}_2$, and confirms the “indirect mechanism” as the dominant path to reach the population of the HS state.

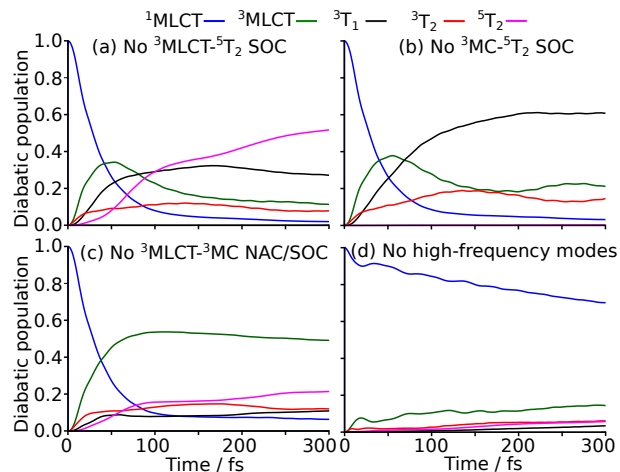


Figure 3: Diabatic population dynamics using different reduced models, namely (a) deactivating the spin-orbit coupling between $^3\text{MLCT}$ and $^5\text{T}_2$, (b) deactivating the spin-orbit coupling between ^3MC and $^5\text{T}_2$, (c) deactivating the couplings between ^3MC and $^3\text{MLCT}$, and (d) not including the high-frequency bipyridine modes.

The deactivation of the $^3\text{MLCT}/^3\text{MC}$ non-adiabatic and spin-orbit couplings lowers the population of the quintet state, proportional to the decrease of the population from the ^3MC states. This suggests, on the one hand, that part of the ^3MC population is transferred directly from the $^1\text{MLCT}$ via intersystem-crossing. In addition, it shows that ^3MC states are also populated from $^3\text{MLCT}$ in an internal conversion process. Finally, we deactivated $^3\text{T}_1/\text{HS}$ or $^3\text{T}_2/\text{HS}$ spin-orbit couplings (see Sec. S3.D of the supporting information). The deactivation of the $^3\text{T}_2/\text{HS}$ does not exhibit significant differences in the HS population, whereas the deactivation of $^3\text{T}_{12}/\text{HS}$ drastically reduces the HS population. Therefore, the $^3\text{T}_1$ is the main intermediate populating the $^5\text{T}_2$ state.

From these quantum dynamics results, one can infer a global first-order kinetic model for the light-induced spin crossover (LISCO) reaction of $[\text{Fe}(\text{bpy})_3]^{2+}$, summarized in Fig. 4. To obtain the rates for each process, the kinetic rates have been optimized to fit the evolution of diabatic populations obtained by the wavepacket dynamics with the full model (for further details, see Sec. S3.B in the supporting information). For a successful first-

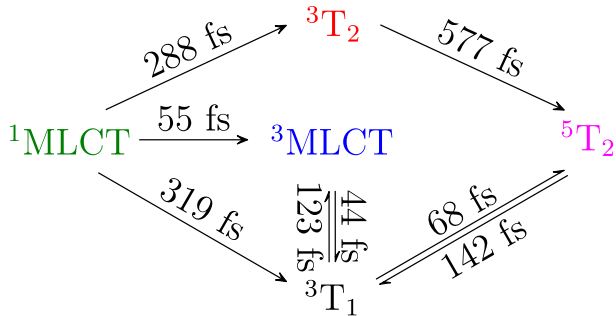


Figure 4: Schematic representation of the kinetic rates extracted from a first-order kinetic model.

order fitting, the back-transfer reactions between ${}^3\text{MLCT}/{}^3\text{T}_1$ and ${}^3\text{T}_1/{}^5\text{T}_2$ are required. Alternatively, such populations can be fitted by adding a delay time in the ${}^3\text{MC}$ states as shown in Ref. 11. On the one hand, the total singlet/triplet transfer takes 40 fs, slightly slower than the < 30 fs transfer observed experimentally.⁵ This transfer can be decomposed in a fast transfer to the triplet MLCT, which takes 55 fs, and two slower transfers directly to the ${}^3\text{T}_1$ and ${}^3\text{T}_2$ MC states in 319 fs and 288 fs, respectively. The total triplet/quintet transfer takes place in 178 fs, in good agreement with the 120-130 fs reported in the literature.^{3-6,8} An equilibrium is established in the triplet MLCT/MC, ${}^3\text{MLCT} \leftrightarrow {}^3\text{T}_1$ with a forward and backward kinetic rate of 44 and 123 fs respectively, thus favoring the population of ${}^3\text{T}_1$. The HS state is populated via a fast decay from the ${}^3\text{T}_1$ state (68 fs) and a slower decay from the ${}^3\text{T}_2$ state (577 fs), further supporting the triplet T_1 as the main state responsible of the transfer to the HS. A back transfer reaction from the HS to the ${}^3\text{T}_1$ states is possible, with a transfer rate of ~~163~~ 142 fs, confirming the ~~picture experimental observation~~ by Gaffney et al. using K_β emission.¹¹

The role of the different vibrational modes in the ultrafast mechanism has been also a matter of discussion.^{7,8} Previous studies agree that the symmetric Fe-N stretching is the dominant mode activated during the LIESST photo process. We confirm this observation from wavepacket dynamics, in which the Fe-N distance is increased by ca. 0.10 Å during the dynamics (see Fig. S11 in SI) due to the popula-

tion of antibonding Fe-N orbitals in MC states. Axial and equatorial Fe-N distances evolve similarly, indicating weak Jahn-Teller distortions. The N-Fe-N bite angle (see Fig. S12 in SI) slightly increases ($\approx 0.5^\circ$) during the first 20 fs of the simulation decreasing steadily to reach a value around -3.0° compared to the LS. The $\text{C}_2\text{-C}_2'$ bond length (see Fig. S13 in SI) initially decreases because of the population of the MLCT states which stabilize at shorter distances because of the π bonding character within the so-called π_1^* orbital. Afterward, it increases as a consequence of the transfer to MC states and the enlargement of Fe-N distances. As stated by Auböck et al.,⁷ the high-frequency modes in bipyridine play a key role in the process. These modes allow an efficient ISC and relaxation in the MLCT band. The exclusion of these modes in reduced model dynamics exhibits a trapped population in the MLCT manifold (see Fig. 3).

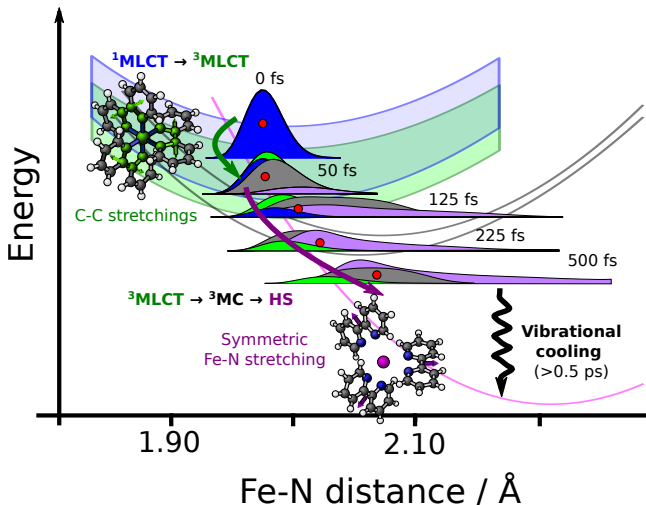


Figure 5: Schematic summary of the photoreaction of $[\text{Fe}^{\text{II}}(\text{bpy})_3]^{2+}$ at key times as determined by quantum dynamics. The wavepacket density along the reaction coordinate is decomposed in the densities of ${}^1\text{MLCT}$ (blue), ${}^3\text{MLCT}$ (green), ${}^3\text{MC}$ (grey), and HS (magenta). The average position is shown as a red circle. The first step is the conversion between MLCTs, dominated by C-C stretchings whereas the MLCT to MC conversion is controlled by the symmetric Fe-N stretchings.

In Fig. 5 we summarize the picture provided by wavepacket dynamics on the LIESST reaction of $[\text{Fe}(\text{bpy})_3]^{\text{II}}$, by showing the wavepacket

density along the reaction coordinate for the first 500 fs of the photoreaction. The intersystem crossing ($^1\text{MLCT} \rightarrow ^3\text{MLCT}$) occurs very rapidly and brings the wavepacket to the bottom of the MLCT band. At this time, a ^3MC population is already appreciable. No activation of the reaction coordinate is observed at this time; bipyridine stretchings exclusively dominate the MLCT relaxation. The numerous vibronic and spin-orbit couplings between the MC/MLCT triplets together with their small energy gap at the $^3\text{MLCT}$ band minimum make the transfer between the two very efficient. However, the compact Gaussian-like wavepacket at the minimum of the MLCT band generates a hot vibrational wavepacket in the direction of the reaction coordinate, as observed by the spreading of the density over a large region of Fe-N distances. This large spread implies that part of the wavepacket is always sitting in a region of efficient transfer between the ^3MC and the HS. After this transfer is complete, the wavepacket rephases at longer times ($> \dot{\tau}$ 0.5 ps) by cooling down by releasing vibrational energy to the environment.

Iron complexes with long-lived charge-transfer states are important for low-cost applications in photocatalysis and solar-cell applications.³² From our dynamics, we observe that the bipyridine $\text{C}_2\text{-C}_{2'}$ stretching is a dominant motion. In fact, the population gets trapped in the MLCT band when excluding these modes from the model. Therefore, one could hypothesize that blocking $\text{C}_2\text{-C}_{2'}$ stretchings in the bipyridine units could produce long-lived MLCT states. To test this, we constructed a new model Hamiltonian, equivalent to the full model, in which we froze the C_2 and $\text{C}_{2'}$ atoms. For the MLCT relaxation, we substituted the $\text{C}_2\text{-C}_{2'}$ stretchings for alternative N-C and C-C stretchings in the bipyridine units. Quantum dynamics simulations with such a model were performed for the singlet and triplet bands, thus excluding the HS state (see Section S4.A in SI). The results show a similar $^1\text{MLCT} \rightarrow ^3\text{MLCT}$ transfer to the dynamics with $\text{C}_2\text{-C}_{2'}$ stretching, indicating that any pyridine stretching mode can contribute to the efficient relaxation of the MLCT and transfer to the MC states.

Therefore, blocking vibrational modes is an inefficient way of controlling the LIESST dynamics.

Alternatively, long-lived charge-transfer states can be obtained by introducing a large energetic gap between the MLCT and MC manifolds, so that the $\text{MLCT} \rightarrow \text{MC}$ transfer becomes inefficient. To test this, we built a new model Hamiltonian of an alternative iron complex, $[\text{Fe}^{\text{II}}(\text{dipyridin-2-ylmethane})_3]^{2+}$, in which the pyridine units are bridged by a methyl group (see Section S4.B in SI). The bridge disrupts the conjugation between the two pyridine rings within the bipyridine unit. As a consequence, the MLCT band is destabilized since the π^* states are higher in energy. On the contrary, the MC states are slightly stabilized because of an increase in the Fe-N distance. We constructed a model including singlet and triplet states along 8 vibrational modes centered on the ligands. Quantum dynamics on the model indicate that the lifetime of the $^1\text{MLCT}$ band becomes 13 ps instead of the 50 fs observed for $[\text{Fe}(\text{bpy})_3]^{2+}$. Therefore, increasing the MC and MLCT gap by ~~destabilizing the π^* orbitals~~ is decreasing the π conjugation of the electron-acceptor ligands might be an efficient way of producing long-lived CT states in iron complexes.

In conclusion, the mechanism of photoinduced spin crossover of $[\text{Fe}(\text{bpy})_3]^{2+}$ has been elucidated by employing quantum wavepacket dynamics simulations on a model Hamiltonian. The model contains all relevant singlet, triplet, and quintet states, expanded on a vibrational space of the symmetric complex expansion (reaction coordinate), several Jahn-Teller modes, and ligand C-C and C-N stretchings. Such a model reproduces the kinetics experimentally reported in several ultrafast optical spectroscopies, including a back-transfer between the HS and the $^3\text{T}_1$ state prior to the final relaxation to the quintet. Comparing the dynamics of the full model with several reduced models, we could unequivocally determine that (i) the triplet $^3\text{T}_1$ state catalyzes the transfer of population to the HS quintet, and (ii) the bipyridine stretching modes have a fundamental role in the sub-ps transfer of population from the MLCT

band to the triplet MC state.

Such findings allowed us to anticipate design strategies for long-lived charge-transfer states in iron complexes. We showed that blocking C₂-C_{2'} bipyridine stretchings is an inefficient way of stabilizing the CT states. On the contrary, increasing the π^* energy by breaking the conjugation between the pyridine units has the effect of increasing the MLCT/MC energy gap. This translates into a 10-fold increase in the MLCT lifetime. These results show the effect that the ligands have in controlling the energy of the MLCT band and the fundamental role of vibrations in the efficiency of ISC to the high-spin.³³

Supporting Information Available

Supporting information contains the computational details for the electronic structure methodology and the analysis vibrational used to construct the model Hamiltonian for $[\text{Fe}^{\text{II}}(2,2'\text{-bipyridine})_3]^{2+}$. In addition, the fitting of quantum dynamics for the full and reduced models to a kinetic model, and the variation of structural parameters is described. Finally, the model construction for $[\text{Fe}^{\text{II}}(\text{dipyridin-2-ylmethane})_3]^{2+}$ is described.

Acknowledgement We acknowledge financial support from the “Agence Nationale pour la Recherche” through the project MULTICROSS (ANR-19-CE29-0018). Centre de Calcul Intensif d’Aix-Marseille is acknowledged for granting access to its high-performance computing resources.

References

- (1) Rusu, I.; Manolache-Rusu, I. C.; Diaconu, A.; Palamarciuc, O.; Gural'skiy, I. A.; Molnar, G.; Rotaru, A. Pressure Gradient Effect on Spin-crossover Materials: Experiment Vs Theory. *J. Appl. Phys.* **2021**, *129*, 064501.
- (2) Hiiuk, V. M.; Shova, S.; Rotaru, A.; Ksenofontov, V.; Fritsky, I. O.; Gural'skiy, I. A. Room Temperature Hysteretic Spin Crossover in a New Cyanoheterometallic Framework. *Chem. Commun.* **2019**, *55*, 3359–3362.
- (3) Gawelda, W.; Cannizzo, A.; Pham, V.-T.; van Mourik, F.; Bressler, C.; Chergui, M. Ultrafast Nonadiabatic Dynamics of $[\text{Fe}^{\text{II}}(\text{bpy})_3]^{2+}$ in Solution. *J. Am. Chem. Soc.* **2007**, *129*, 8199–8206.
- (4) Bressler, C.; Milne, C.; Pham, V.-T.; ElNahas, A.; van der Veen, R. M.; Gawelda, W.; Johnson, S.; Beaud, P.; Grolimund, D.; Kaiser, M. et al. Femtosecond XANES Study of the Light-Induced Spin Crossover Dynamics in an Iron(II) Complex. *Science* **2009**, *323*, 489–492.
- (5) Cannizzo, A.; Milne, C.; Consani, C.; Gawelda, W.; Bressler, C.; van Mourik, F.; Chergui, M. Light-induced Spin Crossover in Fe(II)-based Complexes: The Full Photocycle Unraveled by Ultrafast Optical and X-ray Spectroscopies. *Coord. Chem. Rev.* **2010**, *254*, 2677–2686.
- (6) Zhang, W.; Alonso-Mori, R.; Bergmann, U.; Bressler, C.; Chollet, M.; Galler, A.; Gawelda, W.; Hadt, R. G.; Hartsock, R. W.; Kroll, T. et al. Tracking Excited-state Charge and Spin Dynamics in Iron Coordination Complexes. *Nature* **2014**, *509*, 345–348.
- (7) Auböck, G.; Chergui, M. Sub-50-fs Photoinduced Spin Crossover in $[\text{Fe}(\text{bpy})_3]^{2+}$. *Nat. Chem.* **2015**, *7*, 629–633.
- (8) Lemke, H. T.; Hartsock, K. S. K. R.; van Driel, T. B.; Chollet, M.; Glowina, J. M.; Song, S.; Zhu, D.; Pace, E.; Matar, S. F.; Nielsen, M. M. et al. Coherent Structural Trapping Through Wave Packet Dispersion During Photoinduced Spin State Switching. *Nat. Commun.* **2017**, *8*, 15342.
- (9) Chastanet, G.; Lorenc, M.; Bertoni, R.; Desplanches, C. Light-Induced Spin

- Crossover – Solution and Solid-state Processes. *C. R. Chim.* **2018**, *21*, 1075–1094.
- (10) Zhang, W.; Kjær, K. S.; Alonso-Mori, R.; Bergmann, U.; Chollet, M.; Fredin, L. A.; Hadt, R. G.; Hartsock, R. W.; Harlang, T.; Kroll, T. et al. Manipulating Charge Transfer Excited State Relaxation and Spin Crossover in Iron Coordination Complexes with Ligand Substitution. *Chem. Sci.* **2017**, *8*, 515–523.
- (11) Kjær, K. S.; Driel, T. B. V.; Harlang, T. C. B.; Kunnus, K.; Biasin, E.; Ledbetter, K.; Hartsock, R. W.; Reinhard, M. E.; Koroidov, S.; Li, L. et al. Finding Intersections Between Electronic Excited State Potential Energy Surfaces with Simultaneous Ultrafast X-ray Scattering and Spectroscopy. *Chem. Sci.* **2019**, *10*, 5749–5760.
- (12) Oppermann, M.; Zinna, F.; Lacour, J.; Chergui, M. Chiral Control of Spin-Crossover Dynamics in Fe(II) Complexes. *Nat. Chem.* **2022**, *14*, 739–745.
- (13) de Graaf, C.; Sousa, C. Study of the Light-Induced Spin Crossover Process of the $[\text{Fe}^{\text{II}}(\text{bpy})_3]^{2+}$ Complex. *Chem. Eur. J.* **2010**, *16*, 4550–4556.
- (14) Domingo, A.; Sousa, C.; de Graaf, C. The Effect of Thermal Motion on the Electron Localization in Metal-to-Ligand Charge Transfer Excitations in $[\text{Fe}(\text{bpy})_3]^{2+}$. *Dalton Trans.* **2014**, *43*, 17838–17846.
- (15) Sousa, C.; de Graaf, C.; Rudavskyi, A.; Broer, R.; Tatchen, J.; Etinski, M.; Marian, C. M. Ultrafast Deactivation Mechanism of the Excited Singlet in the Light-Induced Spin Crossover of $[\text{Fe}(2,2'\text{-bipyridine})_3]^{2+}$. *Chem. Eur. J.* **2013**, *19*, 17541–17551.
- (16) Sousa, C.; Llunell, M.; Domingo, A.; de Graaf, C. Theoretical Evidence for the Direct $^3\text{MLCT-HS}$ Deactivation in the Light-induced Spin Crossover of Fe(II)-polypyridyl Complexes. *Phys. Chem. Chem. Phys.* **2018**, *20*, 2351–2355.
- (17) Liu, L. C. *Photoinduced Spin Crossover in Iron(II) Systems*; Chemistry in Action: Making Molecular Movies with Ultrafast Electron Diffraction and Data Science; Springer International Publishing: Cham, Switzerland, 2020; pp 105–161.
- (18) Alías-Rodríguez, M.; Huix-Rotllant, M.; de Graaf, C. Quantum Dynamics Simulations of the Thermal and Light-induced High-spin to Low-spin Relaxation in $\text{Fe}(\text{bpy})_3$ and $\text{Fe}(\text{mtz})_6$. *Faraday Discuss.* **2022**, *237*, 93–107.
- (19) Penfold, T. J.; Gindensperger, E.; Daniel, C.; Marian, C. M. Spin-Vibronic Mechanism for Intersystem Crossing. *Chem. Rev.* **2018**, *118*, 6975–7025.
- (20) Pápai, M.; Penfold, T. J.; Møller, K. B. Effect of tert-Butyl Functionalization on the Photoexcited Decay of a Fe(II)-N-Heterocyclic Carbene Complex. *J. Phys. Chem. C* **2016**, *120*, 17234–17241.
- (21) Pápai, M.; Vankó, G.; Rozgonyi, T.; Penfold, T. J. High-Efficiency Iron Photosensitizer Explained with Quantum Wavepacket Dynamics. *J. Phys. Chem. Lett.* **2016**, *7*, 2009–2014.
- (22) Falahati, K.; Tamura, H.; Burghardt, I.; Huix-Rotllant, M. Ultrafast Carbon Monoxide Photolysis and Heme Spin-crossover in Myoglobin via Nonadiabatic Quantum Dynamics. *Nat. Comm.* **2018**, *9*, 4502.
- (23) Pápai, M.; Abedi, M.; Levi, G.; Biasin, E.; Nielsen, M. M.; Møller, K. B. Theoretical Evidence of Solvent-Mediated Excited-State Dynamics in a Functionalized Iron Sensitizer. *J. Phys. Chem. C* **2019**, *123*, 2056–2065.
- (24) Al-Salka, Y.; Granone, L. I.; Ramadan, W.; Hakki, A.; Dillert, R.; Bahnemann, D. W. Iron-based Photocatalytic and Photoelectrocatalytic Nanostructures: Facts, Perspectives, and Expectations. *Appl. Catal. B* **2019**, *244*, 1065–1095.

- (25) Lawson Daku, L. M.; Vargas, A.; Hauser, A.; Fouqueau, A.; Casida, M. E. Assessment of Density Functionals for the High-Spin/Low-Spin Energy Difference in The Low-Spin Iron(II) Tris(2,2'-bipyridine) Complex. Chemphyschem **2005**, 6, 1393–1410.
- (26) Berger, R. M.; McMillin, D. R. Ultraviolet and Visible Resonance Raman Spectroscopy of tris-(2,2'-bipyridyl) Iron(II): Intensity Considerations and Band Assignments. Inorg. Chim. Acta **1990**, 177, 65–69.
- (27) Braterman, P. S.; Song, J.-I.; Peacock, R. D. Electronic Absorption Spectra of the Iron(II) Complexes of 2,2'-Bipyridine, 2,2'-Bipyrimidine, 1,10-Phenanthroline, and 2,2':6',2''-Terpyridine and their Reduction Products. Inorg. Chem. **1992**, 31, 555–559.
- (28) Zhang, K.; Ash, R.; Girolami, G. S.; Vura-Weis, J. Tracking the Metal-Centered Triplet in Photoinduced Spin Crossover of $\text{Fe}(\text{phen})_{32}^{+}$ with Tabletop Femtosecond M-Edge X-ray Absorption Near-Edge Structure Spectroscopy. J. Am. Chem. Soc. **2019**, 141, 17180–17188.
- (29) McCusker, J. K.; Walda, K. N.; Dunn, R. C.; Simon, J. D.; Magde, D.; Hendrickson, D. N. Subpicosecond $^1\text{MLCT} \rightarrow ^5\text{T}_2$ Intersystem Crossing of Low-Spin Polypyridyl Ferrous Complexes. J. Am. Chem. Soc. **1993**, 115, 298–307.
- (30) Moguelevski, A.; Wilke, M.; Grell, G.; ; Bokarev, S. I.; Aziz, S. G.; Engel, N.; Raheem, A. A.; Kehn, O.; Kiyani, I. Y. et al. Ultrafast Spin Crossover in $[\text{Fe}^{II}(\text{bpy})_3]^{2+}$: Revealing Two Competing Mechanisms by Extreme Ultraviolet Photoemission Spectroscopy. Chem. Phys. Chem. **2017**, 18, 465–469.
- (31) Iuchi, S.; Koga, N. Ultrafast Electronic Relaxation in Aqueous $[\text{Fe}(\text{bpy})_3]^{2+}$: A Surface Hopping Study. J. Phys. Chem. Lett. **2023**, 14, 4225–4232.
- (32) Shepard, S. G.; Fatur, S. M.; Rappé', A. K.; Damrauer, N. H. Highly Strained Iron(II) Polypyridines: Exploiting the Quintet Manifold To Extend the Lifetime of MLCT Excited States. J. Am. Chem. Soc. **2016**, 138, 2949–2952.
- (33) Paulus, B. C.; Adelman, S. L.; Jamula, L. L.; McCusker, J. K. Leveraging Excited-state Coherence for Synthetic Control of Ultrafast Dynamics. Nature **2020**, 582, 214–218.